



Ferromagnetically modified zeolite catalysts for liquid-phase High-Throughput Experimentation

Paolo P. Pescarmona^{1,*}, Bogdan C. Gagea¹, Peter Van der Aa, Pierre A. Jacobs, Johan A. Martens

Centre for Surface Chemistry and Catalysis, University of Leuven (K.U. Leuven), Kasteelpark Arenberg 23, 3001 Heverlee, Belgium

ARTICLE INFO

Article history:

Available online 13 February 2010

Keywords:

High-Throughput Experimentation
Catalyst separation
Magnetic zeolites
Iron-zeolites
Benzylation

ABSTRACT

A novel method for the separation of heterogeneous catalysts from liquid-phase reactions in High-Throughput Experimentation (HTE) libraries was developed based on a magnetic recuperation procedure. Ferromagnetic iron nanoparticles were introduced in a set of zeolite structures by means of aqueous impregnation of an iron precursor, followed by reduction in H₂. The obtained magnetic zeolites can be efficiently stirred in the catalytic reaction mixture using conventional magnetic stirring bars and they are automatically separated by depositing on the magnetic bar when the stirring is stopped. Characterization techniques demonstrated that the iron nanoparticles are distributed on the external surface of the zeolites, where the interference with the catalytic active sites is limited. Catalytic tests of a High-Throughput library of 10 wt. % Fe magnetic zeolites, performed using the liquid-phase benzylation of toluene with benzyl alcohol as test reaction, showed that the modified catalysts can be very easily and efficiently separated from the reaction mixture while they retain similar activity and selectivity to that of the unmodified samples.

© 2010 Elsevier B.V. All rights reserved.

1. Introduction

High-Throughput Experimentation (HTE) techniques find an increasing number of applications in areas such as catalyst preparation and testing [1–7]. Their use in homogeneous catalysis proved to be straightforward due to the similarities with drug discovery approaches. HTE in heterogeneous catalysis had a relatively slow start, partly due to specific problems related to the heterogeneity of the systems, viz. the requirement of solids removal from the reaction medium before sampling from liquid-phase batch reactors or liquids-solids separation before catalyst regeneration [8]. Moreover, many sequences of unit operations in catalyst preparation, such as ion exchange, impregnation, washing, drying, and calcination, require intermediate separation of liquid from solid phase, viz. centrifugation and/or filtration steps, which are difficult to automate and to apply with catalyst libraries. Therefore, HTE with heterogeneous catalysts has been focusing on applications related to gas phase reaction systems, reports of liquid-phase testing of heterogeneous catalysts still being scarce [1,9–14].

Sampling in time from a batch reactor allows extracting the kinetic parameters that form the necessary basis for ultimately

determining the relation with catalyst properties and the reaction mechanism. In absence of efficient solid-liquid phase-separation procedures, only limited data can be obtained for each catalyst in the library. Reported attempts to circumvent this problem consist in sampling a very small volume from the reaction mixture containing invariably also small amounts of solid catalyst, followed by direct chromatographic analysis [15]. Such procedure may result in the undesired accumulation of catalyst in the chromatographic pre-column. Alternatively, it has been proposed to run a parallel set of identical reactions for different reaction times [16]. HTE equipment that allows fully automated catalyst preparation and on-line sampling in combination with fast chromatographic analysis would need fast and efficient liquid-solid separation to achieve optimum performance. In this context, an ideal solution would be represented by a catalyst that automatically separates from the reaction mixture as stirring is stopped. This can be achieved by magnetic separation, which therefore represents a technically attractive alternative to centrifugation or filtration. The preparation of magnetically separable ordered mesoporous carbons and mesostructured silica with surface grafted magnetic cobalt particles has been previously achieved [17,18]. Here, we describe the preparation of magnetic zeolite catalysts, enabling straightforward, fast and adequate separation of a solid catalyst from a batch catalytic reactor. At an HTE level, this methodology allows separation of catalysts in parallel vessels by their collection on the magnetic element upon stopping of the agitation. By restarting the stirring, the catalysts

* Corresponding author. Tel.: +32 16 321592.

E-mail address: paolo.pescarmona@biw.kuleuven.be (P.P. Pescarmona).

¹ These authors contributed equally to this work.

can be rapidly redispersed in the reaction mixture. This approach could also allow the establishment of a (small scale) stable fluidized catalytic bed. Obviously, this technique requires the use of heterogeneous catalysts exhibiting ferromagnetic properties or incorporation of ferromagnetic particles in a solid catalyst. Some authors reported on the magnetic modification of potential catalytic materials with magnetic particles, viz. composites consisting of NaY zeolite and Fe oxide, [19,20], carbon encapsulated Ni-Fe alloy particles [21] and chirally modified Pt supported on silica-coated Fe_3O_4 as catalyst for asymmetric hydrogenation [22].

In the present work, acid zeolites are ferromagnetically modified by means of incorporation of iron particles and tested in the Friedel-Crafts benzylation of toluene. Comparison of acid zeolite catalysts with different topologies in the original and magnetically modified form allowed to establish the validity of the proposed modification method for solids separation in batch reactors in an HTE set-up. The liquid-phase Friedel-Crafts benzylation of toluene was chosen as a test reaction due to the possibility of obtaining various *ortho*-, *meta*-, *para*- product distribution on each of the tested zeolite topologies [23]. HTE was used in order to identify the optimum zeolite for maximizing the yield for each individual mono-alkylated product. The products of the benzylation of toluene are industrially important compounds used as intermediates for pharmaceutical products and in fine chemistry [24]. Liquid-phase Friedel-Crafts alkylations either require up to stoichiometric amounts of Lewis acid catalysts such as AlCl_3 and BF_3 , or alternatively catalytic amounts of acid zeolites, viz. for alkylaromatics production [25]. The shape selective properties characteristic of zeolites can allow driving the reaction selectivity towards a desired isomer [26]. Since zeolites can be synthesized in a large number of topologies, each with specific pore size, pore architecture, and widely varying composition and thus acid strength, the determination of the most suitable zeolite catalyst for a chosen reaction is significantly faster and more efficient with an HTE approach.

2. Experimental

2.1. Materials

Commercially available zeolites: HY PY-44/1C (Si/Al = 2.5) from Zeocat; NaY CBV100 (Si/Al = 2.6), USY CBV600 (Si/Al = 2.8), USY CBV712 (Si/Al = 5.8), USY CBV720 (Si/Al = 13), USY CBV760 (Si/Al = 30) and USY CBV780 (Si/Al = 37) from PQ; HMOR ZM980 (Si/Al = 100) from Zeocat; HBeta CP81BL-251 (Si/Al = 25) from PQ; HZSM-5 (Si/Al = 50) from Degussa. These zeolites were impregnated with an aqueous solution of $\text{Fe}(\text{NO}_3)_3 \cdot 9\text{H}_2\text{O}$ with different concentrations and constant volume of 1 ml per gram of zeolite. The samples were dried at 60 °C in air, and subsequently heated at 400 °C in oxygen for 1 h (heating ramp: 5 °C/min), then in nitrogen for 30 min (to prevent the explosive reaction between O_2 and H_2), and finally in hydrogen for 1 h. Under these conditions, the Fe_2O_3 oxide stemming from calcined $\text{Fe}(\text{NO}_3)_3$, is reduced by H_2 to metallic iron, which is dispersed in the zeolite crystals, yielding zeolite/iron composites.

As an alternative to the impregnation route, magnetically modified zeolites were synthesized by precipitation of iron oxides with a 1 M NaOH solution following a method reported by Oliveira et al. [19]. Another approach consisted in dispersing both zeolite crystals and ferromagnetic particles in a silica matrix that acts as a binder: first, Fe nanoparticles covered in a protective Ni shell were prepared according to a procedure published by Yang et al. [27]; then, a composite material containing 10 wt. % of these Fe/Ni nanoparticles and 25 wt. % of ZSM-5 crystals, was prepared using a previously reported method [28].

2.2. Magnetic recuperation procedure

Samples of the zeolite/iron composites were introduced in an acetone containing glass vial and stirred for 10 min on a magnetic stirring plate at room temperature. As soon as the stirring was stopped, an external magnet was used to attract the composite to the wall of the vial (Fig. 1). After removal of the solvent with a syringe, the glass vial with catalyst was dried in an oven at 90 °C for 12 h. The total weight of the vial with catalyst allowed the determination of the magnetic separation efficiency. Repetition of this cycle for three more times, unequivocally proved the efficiency of the separation of magnetic zeolites from solvent or reaction medium.

2.3. High-Throughput testing

A catalytic test with magnetic recuperation was performed using a Genesis RSP-100 liquid-handling robot equipped with a stirring and heating reaction block with 60 parallel wells [8]. A library of dry zeolite samples was impregnated with Fe^{3+} solution. Impregnation of 0.1 ml of the ferric nitrate stock solution to 100 mg of dry zeolite was done in 10 ml glass vials, followed by drying. Calcination and reduction under H_2 were done in a separate oven. The final catalysts had a 10 wt. % Fe. In the benzylation experiments, magnetic stirrers (12×4.5 mm bar-shaped magnets encapsulated in PTFE with a permanent magnetic field of 15–25 mT) were rotated at 500 rpm, causing good dispersion of the magnetic zeolite (110 mg) in the reaction medium in each HTE vial. When the stirring was stopped, the zeolite powder was rapidly and quantitatively collected at the surface of the permanent magnets. In a typical catalytic test, each 10 ml reactor containing a zeolite sample and a magnetic stirring bar was sealed with a rubber cap. After addition of 5 ml of toluene via the robot, the library of samples was heated to the reaction temperature (80 °C), followed by addition of the second reactant (benzyl alcohol; 1 mmol). Separation of the catalyst from the reaction medium when stopping the magnetic stirring, followed by sampling via septum piercing and transfer to a 98 position GC-rack, took around 17 s for each reactor. The sampling volume was set at 50 μl (1% of total volume) in order to allow multiple sampling steps without causing a significant decrease of the volume of the reaction medium. Sampling was performed at 1, 3, 6, 10 and 15 h reaction time. Sample analysis was performed on a Thermo Finnigan Ultra Fast GC, equipped with a very low volume capillary column (FT: 0.1 μm ; L: 5 m; i.d.: 0.1 mm), the analysis time for each sample being 3 min (starting temperature 125 °C; 25 °C/min up to 175 °C; 150 °C/min up to 250 °C; dwell for 0.5 min).

2.4. Characterization

The type of crystalline phase of the zeolites was confirmed by powder X-ray diffractometry (XRD) analysis on a STOE StadiP diffractometer. TEM investigations were performed with a Phillips

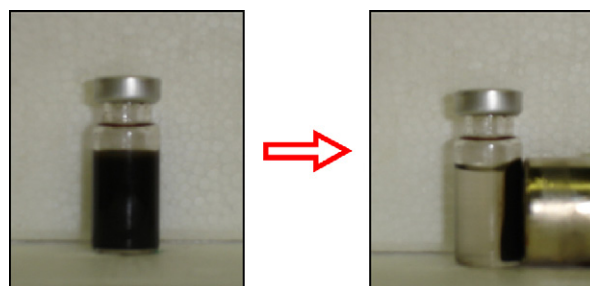


Fig. 1. Magnetic separation procedure.

Table 1
Magnetic recuperation of modified zeolites.

Catalyst	Weight loss per recuperation cycle (wt. %)		
	1	2	3
NaY/Fe ₂ O ₃ ^a	9	4	2
NaY/Fe ₃ O ₄ ^a	5	2	2
NaY/Fe ^a	0	0	0
HZSM-5/FeNi ^b	34	24	–
HZSM-5/2%Fe ^c	5	2	0
HZSM-5/5%Fe ^c	1	0	0
HZSM-5/10%Fe ^c	0	0	0

^a Prepared according to Ref. 19, with 25 wt. % Fe₂O₃.

^b Prepared according to Ref. 27 and 28.

^c Prepared according to the proposed impregnation method.

CM20 operated at 200 kV. Nitrogen adsorption experiments at 77K were carried out with TRISTAR 3000 apparatus from Micrometrics, equipped with three parallel tubes; the samples were pretreated under N₂ flow for 12 h at 200 °C before the measurement. Thermogravimetric analysis (TGA) was performed in either oxygen or hydrogen atmosphere using a TGA Q500 instrument from TA Instruments-Waters LLC.

3. Results and discussion

3.1. Magnetic recuperation procedure

The first step of this work consisted in identifying the most suitable method to prepare the magnetic zeolites. In a first approach, a commercially available NaY zeolite was modified by precipitation of iron oxides from an aqueous iron salt solution by drop wise addition of a 1 M NaOH solution [19]. After drying and calcination at 400 °C iron oxide/H-zeolite ferromagnetic composites showed a loss of solid in each magnetic recuperation test (with a 0.3 T magnet) (Table 1). Only after subsequent hydrogen reduction at 400 °C, full magnetic recuperation of the solid was possible during several consecutive re-slurring steps of the solid in the reaction medium. An alternative method based on immobilization of ferromagnetic nanoparticles by binding both zeolite and ferromagnetic particles in a silica matrix failed to produce solids that could be recovered magnetically (Table 1). The best results were obtained using an impregnation method, which enabled to find the minimum Fe loading necessary to achieve full magnetic recuperation. Different Fe loadings were tested on a HZSM-5 zeolite using the impregnation procedure described in Section 2.1: although 5 wt. % Fe showed a very good recuperation potential with the 0.3 T magnet, for reaching 100% recovery using magnetic stirring bars (magnetic field of 15–25 mT) a minimum iron content of 10 wt. % was required (Table 1 and Fig. 1). The impregnation method was selected to prepare a library of different types of ferromagnetically modified zeolites.

3.2. Characterization of the ferromagnetically modified zeolites

Figure 2 shows a TEM picture of the HZSM-5 sample modified with 10 wt. % of iron by the impregnation method. The dark spots present on the zeolite crystals have been identified as iron particles by EDX analysis. The iron particles have an average size of ~10 nm, implying that they are too large to fit inside the zeolite micropores. Therefore, it was concluded that the iron particles are located on the exterior surface of the zeolite crystals, where the interference with the catalytic active sites is limited. The iron particles were homogeneously distributed on all zeolite crystals in line with the 100% solid recovery potential.

In order to assess the structural integrity of the zeolite in the composite, the ferromagnetically modified materials were charac-

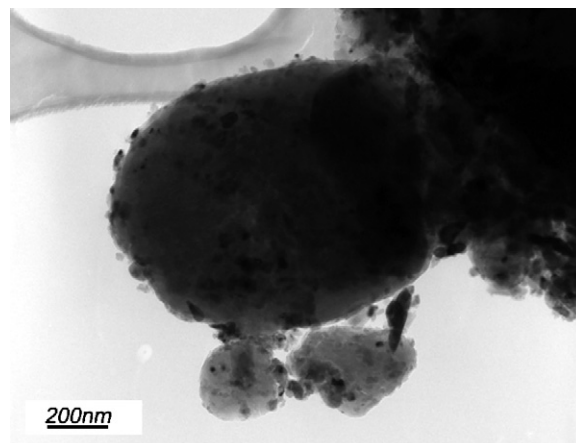


Fig. 2. TEM picture of a HZSM-5/10%Fe composite.

terized using nitrogen physisorption and the results were compared to those of unmodified zeolites (Table 2). BET surface area and micropore volume are practically unaffected in HZSM-5 with 2% of reduced iron. However, a decrease in the BET surface area and micropore volume was observed for all H-zeolites with the higher loading of reduced iron required for an efficient magnetic separation (5 and 10%), suggesting that the access to a small fraction of the micropores is blocked by the iron nanoparticles. Between the oxidation and reduction step, there occurs an increase in both surface area and pore volume relative to the same zeolite mass (Table 2, entry 2 and 3). This behavior can be explained by the migration of iron particles from the interior of the microporous system towards the external surface of the crystal,

Table 2
Nitrogen physisorption on iron-zeolite composites.

Catalyst	BET (m ² /g) ^a	V _{mp} (ml/g) ^a
HZSM-5	495	0.23
HZSM-5/14%Fe _x O _y ^b	366	0.15
HZSM-5/10%Fe ^c	450	0.20
HZSM-5/5%Fe ^c	436	0.20
HZSM-5/2%Fe ^c	495	0.22
HMOR	428	0.16
HMOR/10%Fe ^c	404	0.15
USY CBV720	555	0.18
USY CBV720/10%Fe ^c	508	0.18

^a BET and micropore volume corrected per gram of zeolite.

^b After calcination.

^c After hydrogen reduction.

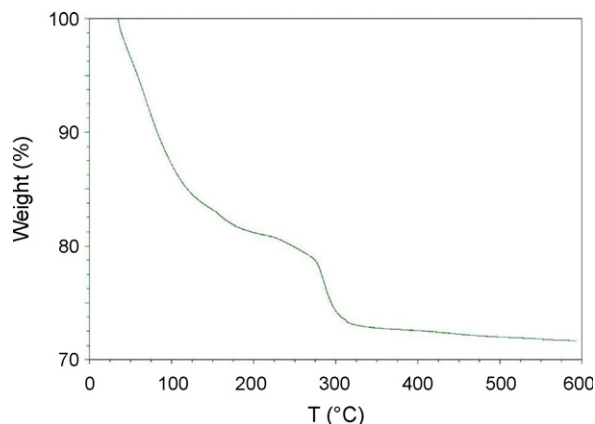
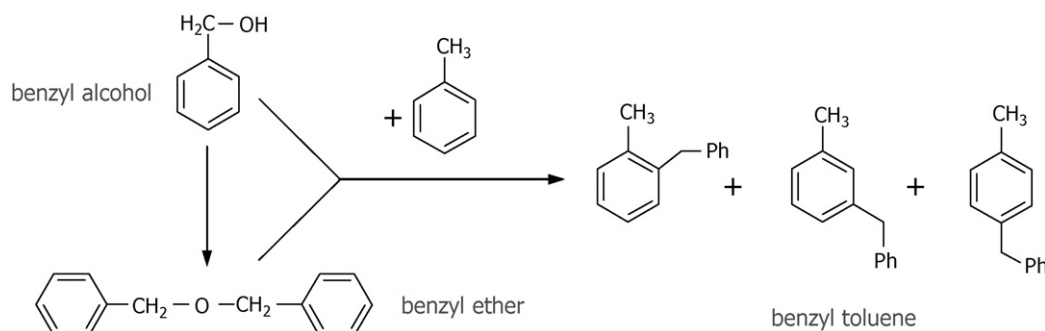


Fig. 3. TGA analysis of NaY/10%Fe under H₂.



Scheme 1. Benzylation of toluene with benzyl alcohol.

thus liberating pores for catalytic reaction. These results are in agreement with the TEM observations. XRD characterization demonstrated that the zeolite frameworks were not affected by the formation of the ferromagnetic particles. Characterization of the iron phase using XRD was hindered due to the overlapping of the highest intensity diffraction line of Fe^0 (44.7 degree 2θ) with reflections from the zeolite frameworks. Experimental confirmation of the formation of a Fe^0 phase stems from *in situ* thermogravimetric hydrogen reduction of a standard Fe_2O_3 . A weight loss step around 290 °C was identified as the reduction of Fe_2O_3 to Fe^0 . A corresponding weight loss step was identified for a NaY/10%Fe zeolite (Fig. 3). Therefore, thermogravimetric data indicate that the 400 °C reduction step efficiently leads to particles of iron in the reduced state (Fe^0).

3.3. Catalytic testing of the ferromagnetically modified zeolites

Once it was determined that an iron loading of 10 wt. % was needed to achieve the desired separability, an HTE library of 10 wt. % Fe zeolites was prepared with the impregnation method and tested together with the corresponding unmodified H-zeolites. Benzylation of toluene with benzyl alcohol (Scheme 1) was chosen as test reaction to compare the Friedel-Crafts activity and selectivity of the ferromagnetically modified H-zeolites with the parent solid acid materials. Possible reaction products are mono-alkylated *ortho*-, *meta*-, and *para*- benzyl toluene isomers, as well as benzyl ether. Di-alkylated products did not form. Thanks to the spontaneous and efficient separation of the ferromagnetically modified zeolites from the reaction mixture upon stopping of the stirring, liquid samples could be directly transferred to a GC using an automated HTE protocol and rapidly analysed. On the other hand, samples from the parent zeolites required a manual filtration step prior to GC analysis.

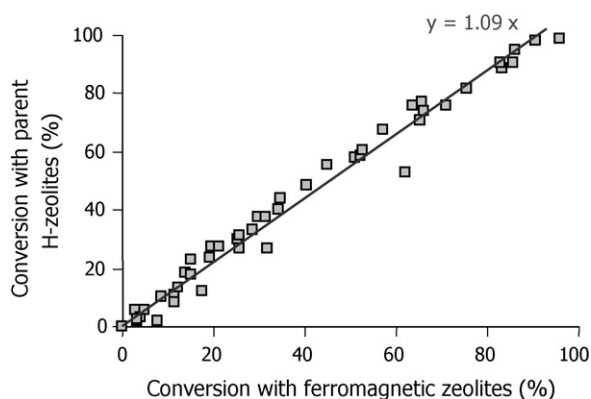


Fig. 4. Benzyl alcohol conversion on H-zeolites vs. ferromagnetically modified H-zeolites.

All the tested ferromagnetically modified H-zeolites showed comparable activity to that of the unmodified samples (Fig. 4 and Table 3). The slope of the straight line through the origin fitting the experimental data is equal to 1.092, pointing to a systematically reduced activity of the iron-loaded H-zeolites by ca. 9%. Although the iron nanoparticles are not active themselves, they can cover some of the active Brønsted acid sites located at the external

Table 3
Benzylation of toluene on ferromagnetically modified and parent zeolites.

Catalyst	Conversion (mol. %) vs. reaction time (h)				
	1	3	6	10	15
HZSM-5/10%Fe	4.1	10.0	15.1	20.3	25.7
HZSM-5	3.4	18.2	18.1	30.0	31.3
HMOR/10%Fe	1.3	34.2	51.2	62.0	86.3
HMOR	5.7	40.3	57.7	82.3	95.1
HBeta/10%Fe	11.5	23.7	37.3	65.6	83.2
HBeta	10.7	33.1	49.7	81.8	88.6
HY/10%Fe	8.6	57.1	65.9	90.8	95.9
HY	10.2	67.5	77.0	98.1	98.8
USY CBV600/10%Fe	3.3	7.6	12.3	25.9	52.3
USY CBV600	1.6	2.0	13.1	26.9	58.5
USY CBV712/10%Fe	3.1	19.3	29.9	52.7	71.2
USY CBV712	2.7	23.4	37.4	60.7	75.6
USY CBV720/10%Fe	11.4	17.5	34.0	67.5	85.9
USY CBV720	8.3	12.3	24.6	46.7	90.2
USY CBV760/10%Fe	15.3	19.5	26.5	65.4	82.7
USY CBV760	23.1	27.2	39.6	70.5	90.2
USY CBV780/10%Fe	4.9	21.1	34.6	40.1	57.8
USY CBV780	5.9	27.3	44.1	60.3	75.6

Table 4
Isomer product distribution in the benzylation of toluene on ferromagnetically modified and parent zeolites.

Catalyst	Isomer distribution (%)		
	<i>Meta</i>	<i>Para</i>	<i>Ortho</i>
HZSM-5/10%Fe	5.3	50.1	44.6
HZSM-5	5.4	49.1	45.5
HMOR/10%Fe	4.0	53.8	42.2
HMOR	4.0	54.4	41.6
HBeta/10%Fe	7.7	25.8	66.5
HBeta	7.8	25.7	66.5
HY/10%Fe	3.9	46.1	50.0
HY	4.1	45.6	50.3
USY CBV600/10%Fe	4.3	43.6	52.1
USY CBV600	4.1	44.8	51.1
USY CBV712/10%Fe	4.2	44.8	51.0
USY CBV712	4.1	44.7	51.8
USY CBV720/10%Fe	4.2	45.1	50.6
USY CBV720	4.0	44.9	51.1
USY CBV760/10%Fe	4.9	44.8	50.2
USY CBV760	4.5	45.1	50.3
USY CBV780/10%Fe	4.5	45.5	50.0
USY CBV780	4.5	45.3	50.2

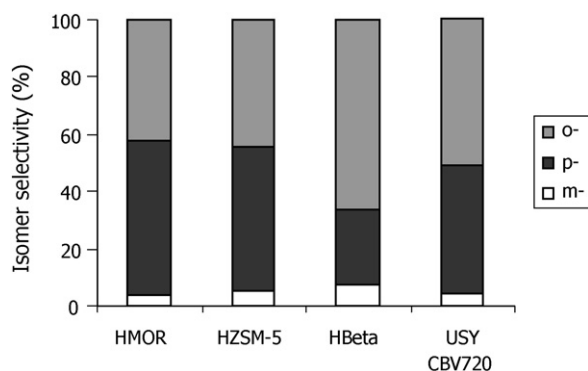


Fig. 5. Mono-alkylated isomer product selectivity on ferromagnetically modified H-zeolites at 5% conversion.

surface and partially block the pore entrances, as indicated by the decrease in BET area and micropore volume observed for the 10 wt. % Fe zeolites (see Section 3.2). The selectivity among the isomers of benzyl toluene produced in the reaction shows an excellent match between the parent zeolites and the corresponding magnetically modified samples (Table 4). This behavior proves that, although the Fe nanoparticles can block some of the active sites resulting in a lower activity, the integrity of the catalytically active site was preserved. Since the catalytic trends observed with the ferromagnetic and with the parent commercial zeolites are similar, it was concluded that the employed High-Throughput approach is suitable to study and compare the performance of libraries of zeolites as catalysts in the benzylation of toluene.

The distribution of mono-alkylated isomers was found to be independent of reaction time on all tested zeolites. The isomer selectivity was determined by the structural properties of the various zeolite frameworks: zeolite Y and all USY (FAU) displayed the same distribution among the three isomers, regardless of their activity (Fig. 5). The high selectivity for the bulky *o*-isomer (66.5%) observed with HBeta zeolite can be related to its large external surface area, while for HZSM-5 and HMOR the high *p*-selectivity (50 and 54%, respectively) is in line with their small pore size. For the large pore size Y and USY zeolites, no selectivity for *o*- nor *p*-isomers was observed. The selectivity data show that the HTE screening of ferromagnetically modified zeolites is sensitive enough to differentiate between various zeolitic structures.

The similarity in selectivity and conversion for the ferromagnetic zeolites and the unmodified commercial zeolites is further illustrated by an identical change of the benzyl ether yield (Fig. 6) for both types of catalysts. Benzyl ether is an intermediate in the benzylation of toluene (Scheme 1). Depending on the zeolite topology, concentration and strength of the acid sites of each zeolite, this intermediate can be formed in different amounts and

further consumed at higher conversions. HBeta zeolite showed the highest yield in di-benzyl ether (41.6%), while the MOR produced the smallest amount (9.8%) at short reaction time (Fig. 6). For all tested zeolites the benzyl ether shows the highest yield at low reaction times and consecutive consumption at increased conversions, pointing to its role as intermediate.

Among the tested zeolites, HY displayed the highest catalytic activity, reaching almost complete conversion of benzyl alcohol after 15 h (Table 3). This result can be attributed to the fact that this zeolite presents the largest pores and the highest concentration of Brønsted acid sites among the tested materials. USY zeolites are H-zeolites with different degree of dealumination, prepared from zeolite Y by steaming and acid leaching treatments. The absolute reactivity sequence (TOF $\times 10^6$, s^{-1} ; first number in brackets) for this series of zeolites was the following:

USY CBV760 (1583; 0.016) > USY CBV780 (808; 0.010) > USY CBV720 (402; 0.047) > USY CBV712 (91; 0.057) > USY CBV600 (82; 0.067)

These results can be discussed in terms of the different concentration (%) of $Al(IV)_{framework}$ measured with MAS NMR ($Al(IV)_{framework}/(Al + Si)$; number in italics in brackets) [29]. Tetrahedrally coordinated framework aluminium sites, $Al(IV)_{framework}$, are generally recognized as the catalytic active Brønsted acid sites in zeolites. The maximum in specific catalytic activity for intermediate $Al(IV)_{framework}$ concentration is in line with the observation made for other acid catalyzed reactions, corresponding to an optimum combination of Brønsted acid site strength and concentration [29].

4. Conclusions

A library of ferromagnetically modified zeolites was prepared by deposition of 10 wt. % Fe nanoparticles on various commercial zeolites. The obtained materials could be separated magnetically at any stage of a catalytic test performed in parallel vessels using a High-Throughput Experimentation set-up. The magnetic separation was instantaneously achieved by switching off the stirring, followed by rapid redispersion when the stirring was switched on again, thus allowing straightforward sampling in time. The effectiveness of the methodology was proved by comparing the catalytic performance of the library of ferromagnetically modified zeolites in the benzylation on toluene with benzyl alcohol with that of the corresponding unmodified zeolites. The magnetic zeolites showed comparable but on average slightly lower activity than the unmodified samples. Such decrease is ascribed to partial blockage of the pore entrances by the iron nanoparticles and to the covering of some of the active Brønsted acid sites located at the external surface. The selectivity among the mono-alkylated isomers obtained with the magnetic zeolites is analogous to that found with the unmodified materials. These results prove that the modification of zeolites by deposition of ferromagnetic particles is an efficient method for enabling the rapid screening of zeolite catalysts by means of HTE. This approach is of general validity and can be used for testing libraries of zeolites in liquid-phase organic reactions in which iron nanoparticles do not display catalytic activity. In order to grant the efficiency of the magnetic separation, it is necessary to avoid conditions in which the iron nanoparticles would get oxidized, thus limiting the range of application of the present method to non-aqueous systems. Future research in this field should be aimed at developing oxidation-resistant magnetic systems.

Acknowledgements

The authors acknowledge sponsoring from IWT (SBO), FWO, GOA, IAP-PAI, VIRCAT, CECAT and long-term structural funding

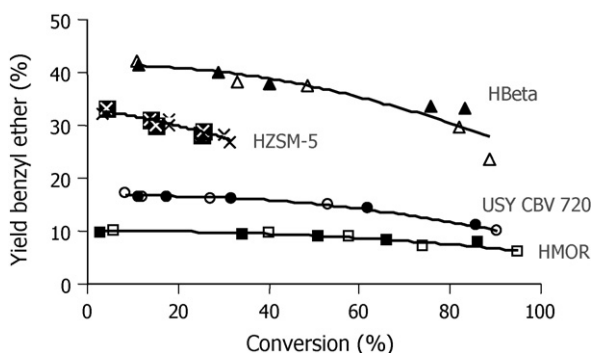


Fig. 6. Benzyl ether yield vs. conversion of benzyl alcohol. Parent H-zeolites: open symbols; ferromagnetically modified H-zeolites: black symbols.

(Methusalem). Dr. Bernard Stuyven is acknowledged for the measurement of the magnetic field. Dr. Duoduo Liang and Prof. Gustaaf Van Tendeloo are acknowledged for the TEM pictures.

References

- [1] A. Hagemeyer, P. Strasser, A.F. Volpe, jr. (Eds.), *High-Throughput Screening in Chemical Catalysis*, Wiley-VCH, Weinheim, 2004.
- [2] B. Jandeleit, D.J. Schaefer, T.S. Powers, H.W. Turner, W.H. Weinberg, *Angew. Chem. Int. Ed* 38 (1999) 2494.
- [3] M.T. Reetz, *Angew. Chem. Int. Ed* 40 (2001) 284.
- [4] S. Senkan, *Angew. Chem. Int. Ed* 40 (2001) 312.
- [5] R.J. Hendershot, C.M. Snively, J. Lauterbach, *Chem. Eur. J* 11 (2005) 806.
- [6] P.P. Pescarmona, J.C. van der Waal, I.E. Maxwell, T. Maschmeyer, *Catal. Lett* 63 (1999) 1.
- [7] W.F. Maier, K. Stöwe, S. Sieg, *Angew. Chem. Int. Ed* 46 (2007) 6016.
- [8] P.P. Pescarmona, K.P.F. Janssen, P.A. Jacobs, *Chem. Eur. J* 13 (2007) 6562.
- [9] A. Guram, A. Hagemeyer, C.G. Lugmair, H.W. Turner, A.F. Volpe Jr., W.H. Weinberg, et al. *Adv. Synth. Catal* 346 (2004) 215.
- [10] A. Corma, J.M. Serra, P. Serna, S. Valero, E. Argente, V. Botti, *J. Catal* 229 (2005) 513.
- [11] P.P. Pescarmona, J. Van Noyen, P.A. Jacobs, *J. Catal* 251 (2007) 307.
- [12] P.P. Pescarmona, P.A. Jacobs, *Catal. Today* 137 (2008) 52.
- [13] G. Stoica, M. Santiago, P.A. Jacobs, J. Pérez Ramírez, P.P. Pescarmona, *Appl. Catal. A* 371 (2009) 43.
- [14] P.P. Pescarmona, K.P.F. Janssen, C. Stroobants, B. Molle, J.S. Paul, P.A. Jacobs, et al. *Top. Catal.* (2010) DOI 10.1007/s11244-009r-r9433-8.
- [15] J.M. Serra, A. Corma, in: A. Hagemeyer, P. Strasser, A.F. Volpe, jr. (Eds.), *High-Throughput Screening in Chemical Catalysis*, Wiley-VCH, Weinheim, 2004, p. 129.
- [16] P.P. Pescarmona, K.P.F. Janssen, C. Delaet, C. Stroobants, K. Houthoofd, A. Philippaerts, et al. *Green Chem.* (2010) in press.
- [17] A.H. Lu, W. Schmidt, N. Matoussevitch, H. Bönemann, B. Spliethoff, B. Tesche, et al. *Angew. Chem. Int. Ed* 43 (2004) 4303.
- [18] A.H. Lu, W.C. Li, A. Kiefer, W. Schmidt, E. Bill, G. Fink, et al. *J. Am. Chem. Soc* 126 (2004) 8616.
- [19] L.C.A. Oliveira, D.I. Petkowicz, A. Smaniotto, S.B.C. Pergher, *Water Res* 38 (2004) 3699.
- [20] A.B. Bourlinos, R. Zboril, D. Petridis, *Micropor. Mesopor. Mater* 58 (2003) 155.
- [21] W. Teunissen, A.A. Bol, J.W. Geus, *Catal. Today* 48 (1999) 329.
- [22] B. Panella, A. Vargas, A. Baiker, *J. Catal* 261 (2009) 88.
- [23] N. Narender, K.V.V. Krishna Mohan, S.J. Kulkarni, I. Ajit Kumar Reddy, *Catal. Comm* 7 (2006) 583.
- [24] Y. Sun, R. Prins, *Appl. Cat. A* 336 (2008) 11.
- [25] J.S. Beck, A.B. Dandekar, T.F. Degan, in: M. Guisnet, J.-P. Gilson (Eds.), *Zeolites for Cleaner Technologies*, Imperial College Press, London, 2002, p. 223.
- [26] P. Marion, R. Jacquot, S. Ratton, M. Guisnet, in: M. Guisnet, J.-P. Gilson (Eds.), *Zeolites for Cleaner Technologies*, Imperial College Press, London, 2002, p. 281.
- [27] C. Yang, J. Xing, Y. Guan, J. Liu, H. Liu, J. Alloys and Compounds 385 (2004) 283.
- [28] B.C. Gagea, D. Liang, G. Van Tendeloo, J.A. Martens, P.A. Jacobs, *Stud. Surf. Sci. Catal* 162 (2006) 259.
- [29] M.J. Remy, D. Stanica, G. Poncelet, E.J.P. Feijen, P.J. Grobet, J.A. Martens, et al. *J. Phys. Chem* 100 (1996) 12440.